Progress in Physics of Applied Materials 6 (2026), Serial Number 13, 343-357

Semnan University

Progress in Physics of Applied Materials

journal homepage: https://ppam.semnan.ac.ir/

A Comprehensive Study on the Synthesis, Nonlinear Optical Properties, and Biological Applications of Substituted Piperazine Derivatives

Sahaya Infant Lasalle B*, Senthil Pandian Muthu, Ramasamy P

Department of Physics, SSN Research Centre, Sri Sivasubramaniya Nadar College of Engineering, Kalavakkam – 603110, Tamil Nadu, India

ARTICLE INFO

Article history:
Received: 18 February 2026
Revised: 6 May 2026
Accepted: 8 May 2026
Published online: 3 June 2026

Keywords:
Piperazine;
Single Crystals;
Single Crystal X-ray diffraction;
Third harmonic generation.

ABSTRACT

Piperazine is an important organic heterocyclic compound featuring a six-membered ring with two nitrogen atoms positioned opposite each other and four carbon atoms. This moiety is present in numerous widely recognized drugs with diverse therapeutic applications, including antipsychotics, antihistamines, antianginal agents, antidepressants, anticancer agents, antivirals, cardioprotective agents, anti-inflammatory drugs, and imaging agents. In addition to members of the thiazole, benzimidazole, and tetrazole families, certain piperazine analogues also exhibit notable pharmacophoric activities. Consequently, many synthesized derivatives exhibit considerable antimicrobial and antifungal properties. This article describes the growth and characterization of piperazine derivative single crystals, which were analyzed using several techniques to evaluate their potential nonlinear optical applications, including structural analysis (single-crystal X ray diffraction), optical studies (UV–Vis–NIR spectroscopy), and Z scan measurements (third harmonic generation), as well as their biological activities, such as anthelmintic, antitumor, anti-inflammatory, and antimycobacterial activities.

1. Introduction

Piperazine and its derivatives represent an important class of heterocyclic compounds that have attracted considerable attention in materials science and pharmaceutical chemistry due to their versatile structural flexibility and wide range of biological activities. These compounds are well known for exhibiting antipsychotic, antihistaminic, anticancer, antiviral, cardioprotective, and anti-inflammatory properties, making them valuable scaffolds in drug design and medicinal applications. Beyond their biological relevance, piperazine derivatives have also emerged as promising candidates in the field of nonlinear optical (NLO) materials because of their ability to form stable crystalline architectures through hydrogen bonding and ionic interactions.

In recent years, single crystals of organic and semi-organic materials have gained significant interest owing to their potential applications in optoelectronic devices, optical switching, frequency conversion, and laser technology. Piperazine-based crystals, in particular, offer advantages such as high optical transparency, good thermal stability, and tunable molecular structures, which are essential for nonlinear optical applications. Despite these advantages, systematic investigations into the growth, structural properties, and optical nonlinearities of many piperazine derivatives remain limited in the literature. Therefore, in the present work, we report the synthesis, crystal growth, and comprehensive characterization of a new piperazine derivative single crystal, focusing on its structural, spectroscopic, thermal, and nonlinear optical properties for potential photonic applications [1].

Piperazines were initially named due to their chemical resemblance to piperidine, a component of piperine found in the black pepper plant (Piper nigrum). In recent years, medicinal chemists have achieved significant success in redesigning this scaffold, which is crucial for achieving precise pharmacological activity. Piperazine derivatives are a diverse class of chemical compounds, many of which

* Corresponding author.
E-mail address: sahayainfant@gmail.com

Cite this article as:

B, S.I.L., Muthu, S.P., P, R., 2026. A Comprehensive Study on the Synthesis, Nonlinear Optical Properties, and Biological Applications of Substituted Piperazine Derivatives. *Progress in Physics of Applied Materials*, *6*(4), pp.343-357. DOI: 10.22075/ppam.2026.40640.1208

possess significant pharmacological properties, and are characterized by a core piperazine heterocyclic nucleus [2].

In terms of hydrogen bonding, piperazine-based materials exhibit a strong tendency to form supramolecular assemblies, which facilitates the development of well ordered crystal structures. Crystalline piperazine adopts a chair conformation, in which the nitrogen atoms participate in N–H interactions located at the equatorial positions, and its structural data are available in the Cambridge Crystallographic Data Centre (CCDC). Piperazine also behaves as an achiral weak organic base, which enhances its versatility in molecular design. Furthermore, high molecular nonlinearity is commonly associated with benzene based derivatives, arising from donor–acceptor substituent groups within the molecular framework.

Materials with a nonlinear optical response can be utilized to manipulate optical signals in various optical devices [3]. Despite extensive research on a wide range of materials, including semiconductors, the development of NLO materials possessing the required properties for specific applications remains an active area of investigation [4]. Recently, optical power limiting, a nonlinear optical effect, has attracted considerable attention because of its potential applications in protecting human eyes and sensitive optical devices from high-intensity laser pulses. Since the discovery of the optical limiting phenomenon, significant efforts have been devoted to the synthesis of new materials with suitable optical limiting properties. Such behavior is primarily attributed to strong nonlinear absorption mechanisms [5].

Antibiotics are a class of medications used to treat a broad spectrum of infections caused by pathogenic microorganisms. They act by disrupting the normal life cycle of bacteria while minimizing harmful effects on human organs and tissues. In recent years, significant research has focused on the use of antibiotics for the treatment of bacterial infections in humans. Nowadays, antibiotics are widely employed in medical practice, including during preoperative and postoperative treatments. In critical procedures, particularly those involving oncology patients, timely antibiotic therapy is administered to prevent secondary infections. Penicillin, discovered in 1928 as the first antibiotic, was soon followed by the introduction of clinically effective sulphonamides. However, the extensive use of penicillin eventually led to the emergence of resistant microbial strains. These penicillin-resistant organisms gradually spread, causing diseases such as pneumonia and thereby reducing the clinical effectiveness of penicillin.

Continuous monitoring and regulation of antibiotic usage have been implemented to control the spread of resistant infections. Nevertheless, such measures are often considered reactive rather than preventive strategies within long-term healthcare planning. Therefore, extensive research efforts are still required to develop novel antibiotic molecules capable of combating bacterial infections effectively. Since bacterial populations continuously evolve and adapt, ongoing investigations and innovative therapeutic approaches remain essential.

Piperazines and their substituted derivatives constitute an important class of pharmacophores. A notable example in this category is indinavir (marketed as Crixivan), which functions as an HIV protease inhibitor. However, piperazinyl cross-linked ciprofloxacin dimers have demonstrated relatively low antibacterial activity against resistant bacterial strains. In contrast, piperazine derivatives linked to benzimidazole and benzotriazole moieties have exhibited significant antifungal activity. Similarly, piperazine derivatives containing a tetrazole nucleus have also been recognized for their antifungal properties.

In the present work, a brief review of piperazine-derivative single crystals and their various characterization techniques is presented. Characterization methods such as single-crystal X-ray diffraction (SCXRD), UV–Visible–NIR spectroscopy, photoconductivity analysis, laser damage threshold measurements, and Z-scan studies are discussed. In addition, the anthelmintic, antitumor, anti-inflammatory, and anti-mycobacterial activities of these compounds are highlighted.

2. Reported Method

2.1. Piperazine Derivatives Act as Various Nonlinear Optical Applications

2.1.1. Single Crystal X-ray Diffraction Analysis

Single-crystal X-ray diffraction (SCXRD) analysis was performed to determine the unit-cell parameters and crystal structure of the piperazine compound. X-ray crystallography is a powerful, versatile, and quantitative technique used to determine the three-dimensional arrangement of atoms and molecules within a crystal. This method is based on the diffraction of X-rays by the periodic atomic arrangement in crystalline materials. The technique produces a three-dimensional electron-density map, which enables the precise determination of crystal structures. It has been widely applied to analyze the structures of numerous organic, inorganic, organometallic, and biological compounds. The crystal structure was solved using single-crystal X-ray diffraction data. The structure solution was obtained by the direct method and subsequently refined by the full-matrix least-squares technique using the SHELXL-97 program package. A summary of the crystallographic parameters obtained from the SCXRD analysis of the novel material is presented in Table 1 [6-15].

2.1.2. Optical Transmittance

Single crystals play a crucial role in various technological applications due to their unique structural and electrical properties. UV–Visible–NIR spectroscopy is a versatile technique that enables the investigation of the optical and electrical behavior of these materials. By analyzing the interaction of electromagnetic radiation with the crystal lattice, this method provides valuable information regarding electronic transitions, bandgap energy, and impurity levels. UV–Visible–NIR spectroscopy is a non destructive technique applicable to a wide range of single crystals, including inorganic, organic, and hybrid materials. This method involves directing a beam of light onto the sample and measuring the intensity of

transmitted or reflected light as a function of wavelength. The resulting spectrum provides detailed information on the material's optical behavior, including its transmission and absorption characteristics. The interaction of light with matter results in transmittance, reflection, and absorption, all of which are affected by the wavelength of the incident light and the crystalline quality of the material.

The optical analysis of grown crystals is crucial for evaluating their suitability for various optoelectronic device applications. Transmittance is a key parameter for materials used in nonlinear optical (NLO) applications. NLO crystals with broad transparency windows are highly advantageous for optical and frequency conversion applications. Revathi Ambika et al [6] reported that Piperazine 1,4 diium bis(2,4 dichlorobenzoate) crystals are transparent throughout the visible region. The UV cut off wavelength was found to be 286 nm, which was attributed to the π→π* electronic transition in the aromatic ring. The absence of absorption between 290 and 800 nm is advantageous for optoelectronic applications, as it indicates good optical transparency and high crystalline quality.

Lasalle et al. [7] investigated the optical properties of the P5NS-grown single crystal. From the UV–Visible spectrum, the cut off wavelength of the P5NS crystal was identified at 400 nm and attributed to π→π* electronic transitions. The transmittance behavior was found to depend strongly on the crystalline quality of the sample. Furthermore, the P5NS crystal exhibited a broad transparent region between 400 and 800 nm without noticeable absorption, indicating its suitability for optical applications.

Lasalle et al. [8] also reported that the PTFA SEST single crystal exhibited a high optical transmittance of 88%, making it suitable for optical device applications. In crystalline materials, an increase in scattering centers generally results in lower transmittance. The high transparency of the PTFA crystal suggests a low dislocation density and reduced scattering centers within the crystal lattice.

The transmittance spectrum of PMC crystals provides important information regarding crystal structure through the interaction of electromagnetic radiation with the material and the associated UV absorption behavior. The absorption observed in the UV region is attributed to n→π electronic transitions caused by the carbonyl functional group present in the compound. Subhashini et al. [13] reported that the absorption maxima observed in the wavelength range of 250–450 nm were associated with electron–phonon anharmonicities, which may enhance the second order optical susceptibility. Subhashini et al [14] also reported that the cut off wavelength of piperazinium (meso)-tartrate single crystals occurred at 270 nm due to electronic excitation within the aromatic system containing nitrogen and hydrogen atoms. This characteristic is highly desirable for crystal based device fabrication.

The UV–Visible spectra of various NLO materials are presented in Figure 1 [1, 6-9, 14], while a summary of the UV–Visible–NIR analysis is provided in Table 2 [6-9, 12, 14, 15].

2.1.3. Photoconductivity Analysis

Photoconductivity is an important phenomenon in solid materials that provides insight into their electronic properties. It describes the var iation in electrical conductivity resulting from the generation or reduction of charge carriers when a material is exposed to radiation under an applied electric field. In the present study, the grown crystals were first coated with a thin silver layer to ensure good electrical contact between the electrodes and the sample. The sample was then placed in a vacuum chamber and connected to a copper electrode.

To measure the dark current (Id), a DC voltage ranging from 0 to 50 V was applied with a gradual increment of 1 V, while the sample was kept in the absence of illumination. Subsequently, the sample was irradiated using a 50 W halogen lamp, and the photocurrent (Ip) was recorded over the same voltage range. The variation of dark current (Id) and photocurrent (Ip) as a function of applied voltage (V) revealed that the photocurrent was consistently higher than the dark current, indicating positive photoconductivity in the material. This behavior arises from the absorption of photons, which increases the number of mobile charge carriers within the crystal. The additional carriers generated upon illumination contribute to the overall current, resulting in enhanced electrical conductivity.

Photoconductive materials can also exhibit a measurable current in the absence of illumination, commonly referred to as dark current. This dark current can significantly influence the accuracy and sensitivity of photoconductivity measurements. In contrast, some materials exhibit negative photoconductivity (NPC), in which the electrical conductivity decreases when the material is exposed to light. This phenomenon is opposite to positive photoconductivity, where illumination increases charge carrier generation and conductivity.

In NPC materials, the decrease in conductivity occurs because the number of free charge carriers available for electrical conduction is reduced under light irradiation. This effect is generally attributed to the presence of defect states, impurity levels, and localized trapping centers within the crystal lattice. Upon illumination, photogenerated electrons and holes may become trapped at these defect sites rather than contributing to electrical conduction. Consequently, the effective concentration of free carriers decreases, resulting in a reduction in photocurrent.

Furthermore, enhanced electron–hole recombination under illumination and increased carrier scattering caused by lattice defects or structural distortions may also contribute to the observed decrease in conductivity. Another possible mechanism involves light induced charge redistribution, which can modify internal potential barriers and hinder carrier transport within the crystal. The extent of negative photoconductivity strongly depends on factors such as defect density, crystalline quality, and the nature of impurity states present in the material. Table 3 [7-9, 16-21, 23-28] represents the photoconductivity analysis of various NLO crystals compared with piperazine derivatives.

Table 1. Summary of novel material single crystal X-ray diffraction analysis.

Crystal Name	Unit cell parameters	Density (Mg/ m^3)	Absorption coefficient	Theta range for data collection	R indices	Crystal size (mm^3)
Piperazine-1,4-diium bis (2, 4 dichlorobenzoate)	a = 11.166(6)Å, b = 8.160(5)Å, c = 12.085(6) Å, α = 90°, β= 113.18(3)°, γ= 90°	1.536	0.612 mm^{-1}	3.189◦ to 34.022°	R1=0.0884, wR2=0.1360	0.150 ×0.15 × 0.100
piperazinium 5-nitrosalicylate	a =6.5815(3) Å, b =7.0392(4) Å, c =10.6813(5) Å, α =95.989(2)◦, β =96.801(2)◦, γ =92.372 (2)◦	1.539	0.128 mm^{-1}	3.315◦ to 28.337◦	R1=0.0444, wR2=0.1255	0.475 ×0.400 ×0.160
Piperazinium bis(trifluoroacetate)	a=6.1290(2)Å, b=7.3849(3)Å, c=7.8982(4)Å, α=62.902(2)°, β=88.825(2)°, γ=78.415(2)°	1.679	0.186 mm^{-1}	2.907 to 28.316◦	R1=0.0732, wR2=0.1986	0.220 ×0.120 ×0.040
Piperazinium mercuric chloride	a =7.5965(3)Å, b=10.5426(4)Å, c=16.1492(6)Å, α=β=γ= 90°	2.396	Multi scan	5.478 to 68.342◦.	R1=0.0274, wR2 =0.0677	0.102 ×0.100 ×0.044
piperazinium perchlorate	a=7.8955(8)Å, b=7.9685(10) Å, c=12.611(2)Å, α=84.587(14) °, β=88.678(14) °, γ= 76.076(10) °		Multi scan			0.21 ×0.19 ×0.15
piperazinium bis(4-hydroxybenzenesulphonate)	a=6.2534(13) Å, b= 6.8951(14)Å, c= 22.259(5) Å, α=γ= 90° , β= 93.62(3) °	1.506	Multi scan	3.26 to 40.24◦	R1=0.0945, wR2=0.1037	0.38 ×0.32 ×0.23
Piperazinium adipate	a= 5.7852 (2) Å, b= 7.4488(2) Å, c= 7.4886 (2) Å, α=64.4690(10)°, β=81.8060(10)°, γ= 80.6600(10)°	1.507	0.104mm^{-1}	3.02 to 24.99°	R1=0.0675, wR2=0.1656	
piperazinium 4-nitrophenolate monohydrate	a=10.9025(4)Å, b=6.2261(3)Å, c=14.0318(5)Å, α=90°, β= 101.286(2)°, γ= 90°	1.424	0.115 mm^{-1}	1.90 to 27.35°	R1 = 0.0486, wR2= 0.1078	0.30 ×0.25 ×0.20
piperazinium (meso)tartrate	a=16.7869(5)Å, b=7.6927(3)Å, c=9.2180(3)Å, α=90°, β= 119.723(2) ° and γ= 90°	1.518	0.130mm^{-1}	2.791-24.99°	R1=0.0306, wR2=0.0951	0.30 ×0.20 ×0.20
Piperazine(bis) p-toluenesulfonate	a=5.9697(3)Å, b=13.1609(7)Å, c=13.6027(7)Å, α=73.665(2)°, β= 85.753(2)°, γ= 83.348(2)°	1.405	0.299 mm^{-1}	1.56 to 34.36°	R1 = 0.0551, wR2= 0.1324	0.24 ×0.20 ×0.18

Negative photoconductivity has attracted considerable attention for various optoelectronic applications, including optical switching, UV/IR sensing, memory devices, and photodetectors, where controlled modulation of electrical conductivity under illumination is required [29, 30].

2.1.4. TGDTA Analysis

Thermogravimetric (TG) and differential thermal (DTA) analyses were carried out on the material to evaluate its thermal stability during the crystal growth process. Figure 2(a) indicates that the present crystal remains thermally stable up to 255 °C. Beyond this temperature, a sharp endothermic peak is observed at 263 °C, corresponding to the decomposition of the P5NS crystal.

Fig. 2(b) shows that the PTFA crystal is thermally stable up to 210 °C, as observed from the TG curve. The decomposition occurs in a single stage, indicating dehydration followed by decomposition of the material [8]. The DTA analysis reveals two distinct endothermic peaks: the first peak at 256 °C corresponds to a phase transition, while the second peak at 276 °C is attributed to the melting point of the PTFA crystal.

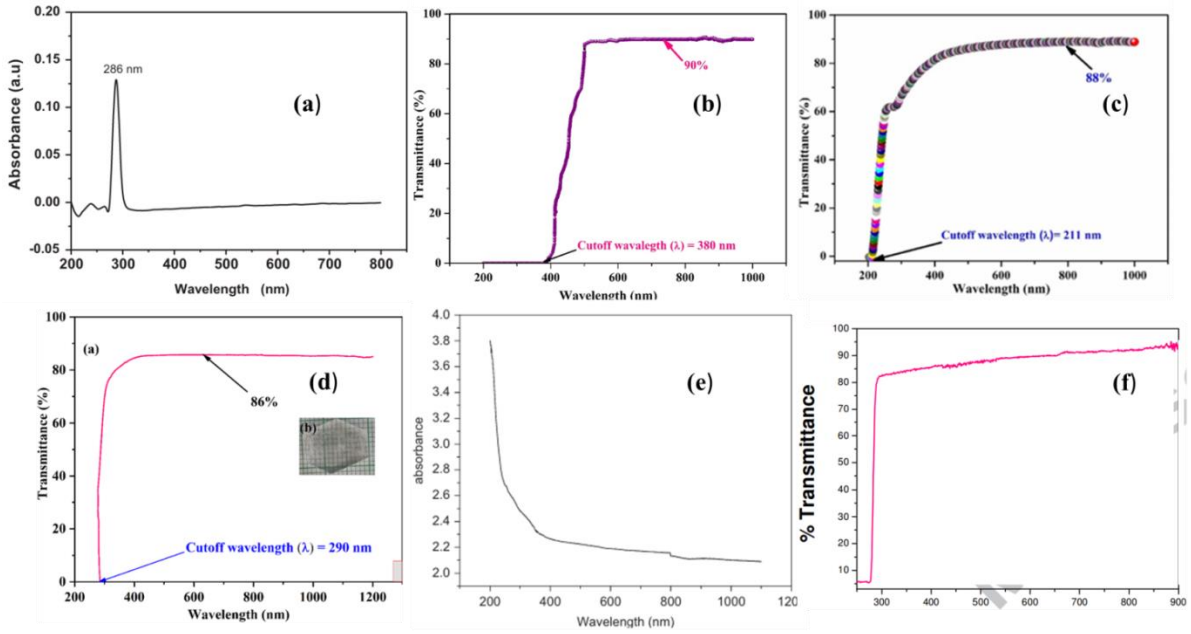

Fig. 1. shows the various NLO material UV-Visible NIR spectra.

Table 2. The summary of UV-Visible NIR analysis.

Crystal Name	Cutoff wavelength	Energy bandgap	Electronic transition	Applications
Piperazine-1,4-dimbis (2, 4-dichlorobenzoate)	286 nm	3.9 eV	π- π∗	optoelectronic device applications
piperazinium 5-nitrosalicylate	380 nm	3.2 eV	π→π*	Optical and frequency conversion application
Piperazinium bis(trifluoroacetate)	211 nm	5.8 eV	n→π*	Harmonic generation and other optical applications
Piperazinium mercuric chloride	290 nm	4.2 eV	n→π*	Optoelectronic applications
Piperazinium adipate	292 nm	4 eV	n→π*	Violet fluorescence emission
piperazinium (meso) tartrate	270 nm	3.8 eV	π →π*	Device fabrication
Piperazine(bis) p-toluenesulfonate	278 nm	4.4 eV	σ → π	Optoelectronic applications

Fig. 2(c) presents the TG and DTA curves of the PTCZM crystal recorded in the temperature range of 30–550 °C. A 1.5 mg crystalline sample was placed in an alumina crucible, and the experiment was carried out at a heating rate of 10 °C min^{-1} under a nitrogen atmosphere to maintain inert conditions. The sharp endothermic peak indicates the high purity and well defined crystalline nature of the sample. From the DTA curve, the peaks observed at 75 °C and 95 °C are attributed to the release of adsorbed water molecules, whereas the peak at 115 °C corresponds to the removal of lattice bound water from the PTCZM crystal. In the PTCZM system, piperazine molecules are strongly coordinated with chlorine atoms bonded to zinc, which contributes to the enhanced thermal stability of the compound. The endothermic peak observed around 355–360 °C is associated with decomposition involving the removal of zinc and chlorine atoms from the crystal structure.

Table 3. Photoconductivity analysis of various NLO single crystals.

Crystal [Reference]	The photoconductive nature of crystal
Piperazinium 5-nitrosalicylate	Positive photoconductivity
Piperazinium bis(trifluoroacetate)	Negative Photoconductivity
Piperazinium mercuric chloride	Positive photoconductivity
1, 2, 3-Benzotriazolium Dihydrogen Phosphate	Positive photoconductivity
2-amino-4,6 dimethylpyrimidine benzoic acid	Positive photoconductivity
3‑amino‑1,2,4‑triazolium benzoate	Negative Photoconductivity
1,2,3-Benzotriazole 4-Hydroxybenzoic Acid	Negative Photoconductivity
Piperazinediium bis (4-aminobenzoate) dihydrate	Negative Photoconductivity
1, 2, 3- Benzotriazole 2-chloro 4 nitrobenzoic Acid	Negative Photoconductivity
1,2,4-triazole p-nitrophthalic acid	Negative Photoconductivity
Piperazinium Tetrachlorozincate Monohydrate	Negative Photoconductivity
1,2,3-Benzotriazole 3,5-dinitrobenzoic acid	Positive Photoconductivity
2-cyanopyridinium salicylate	Positive Photoconductivity
Anthracene	Positive Photoconductivity
potassium hydrogen phthalate	Positive Photoconductivity
2‑amino 4,6‑dimethyl pyrimidine 4‑nitrophenol	Negative Photoconductivity

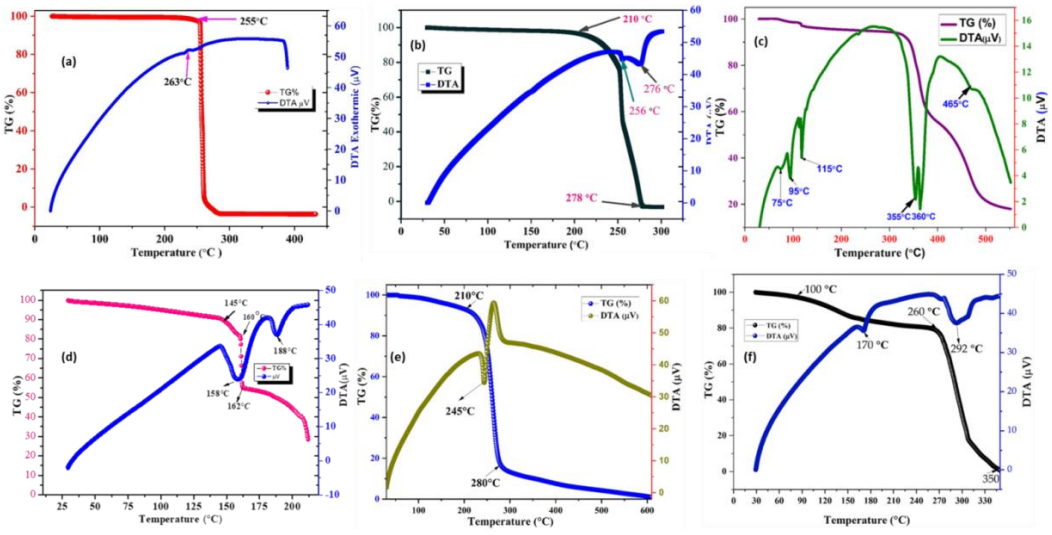

Fig. 2. TGDTA analysis of Piperazine derivative single crystals.

The P4AB crystal is thermally stable up to approximately 145 °C, after which three stages of weight loss are observed, as shown in Figure 2(d). The TG curve indicates an initial mass loss of approximately 9% in the

temperature range of 145–160 °C. The decomposition of the P4AB crystal occurs predominantly in a single stage around 162 °C. In the DTA curve, the first endothermic peak observed at 158 °C corresponds to the melting of the material, while the second peak at 188 °C is associated with the decomposition process. The presence of sharp endothermic peaks confirms the purity and well defined crystalline nature of the sample. Overall, the TG–DTA analysis indicates that the P4AB crystal remains thermally stable up to 145 °C. Furthermore, strong hydrogen bonding interactions within the P4AB structure promote close molecular packing, thereby enhancing its thermal and mechanical stability.

The P2NA crystal exhibits moderate thermal stability up to approximately 210 °C. The DTA curve shows an endothermic peak at 245 °C, while decomposition of the crystal is observed around 280 °C, as illustrated in Figure 2(e).

Fig. 2(f) shows the TG and DTA curves of the PSM crystal. Thermal decomposition occurs in a single stage, beginning at approximately 100 °C and ending around 350 °C, with a total mass loss of nearly 100%. This decomposition is accompanied by the evolution of volatile species such as NO_2, NO, CO_2, and CH, as reported in the literature. No appreciable weight loss is observed in the temperature range of 30–100 °C, indicating that the crystal is thermally stable up to approximately 100 °C. The DTA curve exhibits a single endothermic peak, suggesting that the decomposition process of the PSM compound occurs over the temperature range of approximately 170–292 °C.

The present TG–DTA analysis of piperazine derived crystals demonstrates their good thermal stability, which is an essential requirement for nonlinear optical (NLO) applications. The investigated crystals remain stable over a relatively wide temperature range, with decomposition generally occurring at higher temperatures than those reported for several organic NLO materials. This enhanced thermal stability can be attributed to strong intermolecular interactions such as hydrogen bonding and ionic coordination within the crystal lattice, which improve molecular packing and structural rigidity. Compared with previously reported NLO crystals, piperazine based derivatives exhibit competitive or superior thermal stability, making them promising candidates for applications in laser systems and high temperature environments. The higher decomposition temperatures and well defined endothermic behavior further confirm their suitability for optoelectronic and photonic applications, where thermal endurance is a critical factor.

2.1.5. Laser Damage Threshold Analysis

The laser damage threshold (LDT) refers to the maximum laser fluence that an optical material can withstand without experiencing irreversible damage at a given wavelength and intensity. It is typically determined by exposing the material to laser radiation under controlled conditions. Since the development of lasers in the 1960s and their widespread applications across various industries, the demand for advanced optical materials for device fabrication has significantly increased. These materials are extensively employed in laser systems and related optical devices. To ensure reliable performance, structural integrity, and long term stability, optical components must be capable of withstanding high intensity laser irradiation while maintaining their functional properties under extreme operating conditions [31,32].

NLO (nonlinear optical) crystals should exhibit high optical transparency, a large laser damage threshold, a wide phase matching angle, and significant nonlinear optical coefficients to be effective in laser and high power frequency conversion applications. The laser damage threshold (LDT) depends on both the intrinsic properties of the material and the characteristics of the incident laser beam, which together determine the operational performance range of the crystal.

For applications in laser and high power frequency converters, NLO crystals must satisfy essential criteria such as high transparency, a high laser damage threshold, and efficient phase matching capability, which are critical for the effective functioning of optical devices [33]. Figure 3 [7, 16, 17, 19, 21, 28, 32-34, 36, 37, 39] shows the various LDT patterns of NLO single crystals.

The laser damage threshold of piperazine derived single crystals plays a crucial role in determining their suitability for advanced photonic and optoelectronic applications. Crystals exhibiting high LDT values can withstand intense laser irradiation without structural degradation, making them promising candidates for high power laser systems. In particular, such materials can be effectively utilized in nonlinear optical devices, optical modulators, and frequency conversion systems where strong laser–matter interaction is required.

Furthermore, high LDT piperazine based crystals may serve as potential materials for optical limiting applications, where they protect sensitive optical components and human eyes from laser induced damage. Their good thermal stability and molecular tunability further enhance their applicability in laser communication systems, optical switching devices, and photonic integrated circuits. In addition, these materials may find use in industrial laser processing and laser fusion technologies, where long term stability under extreme irradiation conditions is essential. Table 4 [7, 16-19, 21, 22, 33, 35-38] represents the LDT values of the piperazine derivative compared with other NLO crystals.

Overall, the high LDT performance of piperazine derived single crystals demonstrates their strong potential for next generation high power laser and nonlinear optical applications.

2.1.6. Third Harmonic Generation

A material with a high third‑order nonlinear optical susceptibility (χ^3) is highly desirable for applications such as optical switching, optical limiting, all‑optical signal processing, and photonic device fabrication, because it indicates a stronger interaction between the incident light field and the electronic polarization of the material. This enhanced nonlinear response enables efficient modulation of light at relatively low input intensities. Conversely, materials with lower χ^3 values exhibit weaker nonlinear

responses and are therefore less suitable for high-performance nonlinear optical applications, although they may still be useful in low-intensity or linear optical systems.

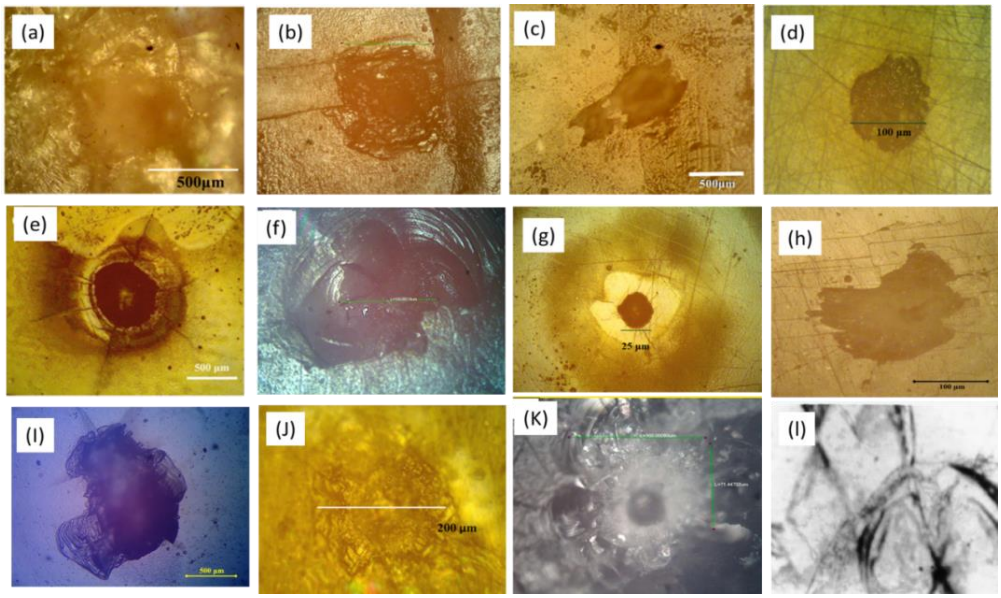

Fig. 3. The LDT patterns of Various NLO single crystals.

Table 4. Laser damage threshold value compared with reported NLO crystals.

Crystal	Laser damage threshold (GW/cm^2)
1,2,3-Benzotriazole 4-Hydroxybenzoic Acid	13.4
1, 2, 3-Benzotriazolium Dihydrogen Phosphate	10.2
Piperazinium 5-nitrosalicylate	8.4
Piperazinium Tetrachlorozincate Monohydrate	7.85
Piperazinium bis(trifluoroacetate)	7.2
1,2,4-triazole p-nitrophthalic acid	6.54
Dilithium succinate	6.25
3-amino-1,2,4-triazolium benzoate	6.12
1,2,3-Benzotriazole 4-chloro-2-Nitrobenzoic acid	6.05
l-proline cadmium chloride monohydrate	4.7
2-amino-4,6-dimethylpyrimidine benzoic acid	4.2
2-amino-4,6-di-methyl-pyrimidinium hydrogen sulfate	3.5

In the present study, the obtained χ^3 value along with the nonlinear refractive index (n_2) and nonlinear absorption coefficient (β) indicates a significant nonlinear optical response arising from molecular charge transfer and electronic polarization effects within the piperazine-based crystal structure. For comparison, the reported χ^3 value is comparable to or higher than those of several previously reported organic NLO materials, including substituted piperazine derivatives, amino acid-based crystals, and other organic charge-transfer complexes. This confirms that the studied crystal exhibits competitive nonlinear optical performance and can therefore be considered a promising candidate for photonic and optical -limiting applications.

The single-beam Z-scan technique is a sensitive and accurate method for determining the nonlinear refractive index (n_2) and nonlinear absorption coefficient (β). One of the major advantages of this method is its ability to simultaneously determine both the magnitude and sign of the nonlinear optical parameters of the sample. The nonlinear refractive index is directly related to the real component of the third-order nonlinear susceptibility, whereas the nonlinear absorption coefficient is associated with its imaginary component [39].

The localized absorption of a tightly focused laser beam on the crystal surface generates a spatial temperature distribution within the material. This temperature variation induces changes in the refractive index, resulting in a thermal lensing effect that distorts the phase of the propagating beam. The difference between the peak and valley transmittance (ΔTp–v) can be expressed in terms of the phase shift at the focal point. From the Z-scan measurements obtained under both open

and closed aperture configurations, the normalized transmittance as a function of sample position enables the determination of both the nonlinear refractive index (n_2) and the nonlinear absorption coefficient (β). Table 5 [7-10, 14, 20, 23, 40] represents the summary of third-order NLO properties.

In the Z‑scan experiment, the sample thickness should be smaller than the Rayleigh length (ZR), which was calculated to be 1.25 mm. The crystal was mounted perpendicular to the sample holder and translated along the laser propagation axis from the negative (−Z) to the positive (+Z) direction. The laser beam was focused using a convex lens with a focal length of 20 cm and directed through the crystal. As the crystal moved along the beam axis, the transmitted intensity varied due to changes in the nonlinear absorption coefficient and refractive index of the material at different positions relative to the focal point. To evaluate the absorption behavior as a function of laser intensity, both open‑ and closed‑aperture configurations were employed during the measurements.

Table 5 presents the nonlinear optical parameters obtained from Z-scan measurements, including the nonlinear absorption coefficient (β), nonlinear refractive index (n_2), and third-order nonlinear susceptibility (χ(3)). These parameters provide direct insight into the third-order nonlinear optical response of the grown crystals. The open-aperture Z-scan results confirm the presence of reverse saturable absorption (RSA) in both crystals, indicating that excited-state absorption dominates over ground-state absorption. This nonlinear absorption mechanism is highly favorable for optical limiting applications, as it enables increased attenuation of high-intensity laser pulses. The closed-aperture Z-scan profiles exhibit a characteristic peak–valley configuration, confirming a negative nonlinear refractive index ($n_2 < 0$), which corresponds to a self-defocusing effect. This behavior arises from intensity-dependent electronic polarization and thermal lensing effects induced under laser excitation. Quantitatively, Piperazinium 5-nitrosalicylate exhibits higher β, n_2, and χ(3) values compared to the cadmium-based complex. The enhanced nonlinear response is attributed to its strong intramolecular charge transfer (ICT) character, extended π-electron conjugation, and efficient donor–acceptor interaction between molecular units. These features significantly increase electronic polarizability and enhance third-order nonlinear susceptibility. In contrast, the cadmium coordination complex shows relatively lower nonlinear coefficients, which is consistent with its localized electronic structure and reduced π-delocalization within the metal–ligand framework. Although its nonlinear response is moderate, it benefits from improved structural stability and higher laser damage threshold, making it more suitable for applications requiring optical robustness. Comparison with reported literature values confirms that both crystals exhibit χ(3) values within the typical range of organic and semi-organic NLO materials, validating the reliability of the measured nonlinear optical response. The observed RSA behavior and negative n_2 values are also consistent with well-established third-order nonlinear optical systems. Overall, the Z-scan analysis demonstrates a clear structure–property relationship, where organic charge-transfer systems favor strong nonlinear optical response, while metal–organic frameworks provide enhanced stability with moderate nonlinearity. This complementary behavior highlights their potential suitability for different classes of photonic and optical limiting applications.

3. Piperazine Derivatives Act as Various Biological Activities

Piperazine is a nitrogen-containing heterocyclic compound. Its core functionality is defined by nitrogen atoms positioned at the 1,4-locations, which can be replaced or modified. Following the initial SN1 reaction, further alkylation and substitution reactions occur. Substituted piperazine derivatives play a crucial role in the development of important drugs. These compounds show a wide range of biological effects, including antitubercular, antibacterial, anti-inflammatory, anticancer, antiviral, antidiabetic, and antimalarial activities. The presence of two nitrogen atoms in the ring allows disubstituted piperazine derivatives to exhibit diverse biological functions. Several newly synthesized 1,4-substituted piperazine compounds were selected based on their biological activity profiles. It is expected that each derivative will display specific biological activities, particularly related to the inhibition of the α-amylase enzyme [41].

In medicinal chemistry, piperazine, also referred to as 1,4-diazacyclohexane, serves as a significant heterocyclic scaffold. It is composed of a six-membered ring with two nitrogen atoms located opposite each other. Piperazine, one of the simplest diazacycloalkanes, plays a vital role in pharmaceutical chemistry due to its ability to generate compounds with diverse biological activities. It wasn't until 1947 that piperazine derivatives gained widespread use as effective treatments for intestinal and tissue-dwelling helminths. However, after researchers at Lederle Laboratories, part of the American Cyanamid Company, discovered the antifilarial properties of 1,4-disubstituted piperazines, these compounds began to be frequently used in the development of important pharmaceuticals [42].

3.1. Anticancer Activity of Piperazine Derivatives

Piperazine derivatives have gained significant attention in medicinal chemistry due to their potential to act as anticancer agents by targeting multiple cellular pathways. The piperazine scaffold is frequently incorporated into drug like molecules because it improves cell permeability, enhances receptor binding flexibility, and contributes to favorable pharmacokinetic properties. Mechanistically, piperazine based compounds exhibit anticancer effects by inhibiting cell cycle progression (particularly G1/S phase arrest), inducing apoptosis (programmed cell death) in cancer cells, interacting with DNA or enzyme targets associated with tumor growth, and suppressing angiogenesis and tumor proliferation signaling pathways.

Table 5. Summary of third order NLO properties.

Name of the Crystals	Piperazinim 5-nitrosalicylate	Piperazinium bis(trifluoroa etate)	piperazinium mercuric chloride	Piperazinium 4-nitrophenolate monohydrate	piperazinium (meso)tartrate crystal	piperazinedi-ium tetrakis (μ2–chloro)-diaqua-dichloro-di-cadmium	Piperazinium Tetrachlorozincate Monohydrate	Piperazinium perchlorate
Laser beam wavelength (λ)	632.8 nm	632.8 nm	632.8 nm	632.8 nm	632.8 nm	632.8 nm	632.8 nm	532 nm
Lens focal length (f)	20 cm	20 cm	20 cm	12 cm	12 cm	20 cm	20 cm	103 mm
Spot-size diameter in front of the aperture(ω_a)	2mm	2mm	2mm	4mm	4mm	2mm	2mm	3.5mm
Aperture radius(r_a)	4mm	4mm	4mm	4mm	4mm	4mm	4mm	1.5mm
Sample thickness	1.5 mm	1.5 mm	1.5 mm	2 mm	2 mm	1.5 mm	1.5 mm	1.5 mm
Effective thickness (L_{eff})	1.75 mm	1.27 mm	1.27 mm	3.57 mm	1.76 mm	1.27 mm	1.27 mm	1.27 mm
Nonlinear refractive index(n_2)	-4.621×10^{-7} cm^2/W	-1.632×10^{-11} cm^2/W	-1.732×10^{-11} cm^2/W	-3.128×10^{-8} cm^2/W	-4.560×10^{-8} cm^2/W	8.675×10^{-11} cm^2/W	-1.632×10^{-11} cm^2/W	1.133×10^{-9} cm^2/W
Nonlinear absorption coefficient (β)	1.272×10^{-4} cm/ W	4.51×10^{-5} cm/ W	0.39×10^{-5} cm/ W	2.15×10^{-3} cm/ W	1.267×10^{-3} cm/ W	4.118×10^{-4} cm/ W	4.51×10^{-5} cm/ W	0.061×10^{-4} cm/ W
Real part of the third-order susceptibility (Re $\chi^{(3)}$)	5.56×10^{-6} esu	1.410×10^{-8} esu	4.69×10^{-7} esu	1.514×10^{-6} esu	1.157×10^{-6} esu	7.745×10^{-9} esu	1.410×10^{-8} esu	0.456×10^{-6} esu
Imaginary part of the third order susceptibility (Im $\chi^{(3)}$))	8.84×10^{-6} esu	1.903×10^{-6} esu	1.573×10^{-6} esu	4.245×10^{-7} esu	1.619×10^{-7} esu	1.900×10^{-7} esu	1.903×10^{-6} esu	0.318×10^{-6} esu
Third- order nonlinear optical susceptibility ($\chi^{(3)}$)	5.56×10^{-6} esu	1.908×10^{-6} esu	4.72×10^{-6} esu	1.548×10^{-6} esu	1.168×10^{-6} esu	1.902×10^{-7} esu	1.908×10^{-6} esu	0.215×10^{-6} esu

Recent studies report that newly synthesized piperazine derivatives show significant cytotoxic activity against several cancer cell lines, including HepG2, indicating their potential as lead compounds for anticancer drug development. For example, Rasheed et al. (2024) demonstrated that novel piperazine derivatives exhibited dose dependent inhibition of HepG2 cancer cell growth, confirming their anticancer potential. Thus, the presence of the piperazine nucleus contributes to strong biological activity through its capability to interact with multiple molecular targets involved in carcinogenesis [43].

3.2. Chemical Properties of Piperazine Compound

Piperazine is a colorless, volatile compound that crystallizes as hexahydrate crystals. It is highly soluble in both organic and aqueous solvents. At 25°C, piperazine exhibits weak basicity, with two pKb values of 9.73 and

5.35. Due to their appropriate alkalinity, ease of modification, ability to form hydrogen bonds, water solubility, and influence on molecular physicochemical properties, piperazine nuclei display a wide range of biological activities [44,45].

3.3. Anthelmintic Agent

Helminthiasis is a condition in which the human body becomes infested with parasitic worms, such as pinworms, roundworms, or tapeworms [46]. These parasites primarily inhabit the gastrointestinal tract; however, they may also migrate to the liver and other organs. Infected individuals excrete helminth eggs in their faces, resulting in soil contamination, particularly in regions with poor sanitation. The anthelmintic properties of piperazine compounds were initially reported in early pharmaceutical studies, and many substituted piperazine derivatives have subsequently demonstrated significant anthelmintic activity [47]. Nevertheless, apart from diethylcarbamazine, only a limited number of these compounds have been adopted for clinical use in human medicine. Piperazine is highly effective against both Ascaris lumbricoides and Enterobius vermicularis. Its primary mechanism of action against Ascaris involves the induction of flaccid paralysis, which facilitates the expulsion of the worm from the body through peristaltic movement. Piperazine hydrate and piperazine citrate are the principal anthelmintic forms of piperazine. These compounds are commonly referred to simply as “piperazine,” which may create confusion between these specific anthelmintic drugs and the broader class of piperazine-based pharmaceutical compounds [48]. Figure 4 shows the chemical structure of flavone and its derivative.

3.4. Antitumor Activity

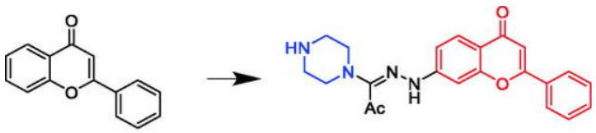

Flavone **1**

Fig. 4. Chemical structure of flavone and its derivative [46].

Abu-Aisheh synthesized a series of N1-(flavon-7-yl) amidrazones, which incorporated N-piperazine groups [49]. According to structure-activity relationships (SARs), the presence of a phenyl group at the C-2 position influences anti-K562 activity. However, none of the compounds with a methyl group at C-2 showed activity against K562 cell lines. In contrast, several compounds from the flavone series (with a phenyl group at C-2) and a few from the 2-methyl series exhibited activity. Anti-K562 activity was more pronounced when the piperazine ring remained unsubstituted, and similar results were observed for anti-T47D activity in breast cancer cells. Compound (Figure 4) demonstrated potential as an antineoplastic agent against T47D breast cancer cells, with an IC50 value of 1.42 μM. Unfortunately, its efficacy is lower compared to doxorubicin, the positive control drug, which has an IC50 of 0.33 μM [50].

3.5. Anti-inflammatory Agent

Inflammation, derived from the Latin word inflamatio, which means "to set on fire," is the intricate biological reaction of vascular tissues to damaging stimuli, including infections, damaged cells, or irritants. It is an attempt by the body to defend itself by removing harmful stimuli and starting the tissue's healing process.

3.6. Anti-mycobacterial Agent

Bacterial infections remain one of the major causes of mortality and morbidity in tropical countries worldwide. Antibiotics are commonly prescribed for the treatment of severe and sometimes life-threatening bacterial infections. However, the rapid emergence of antibacterial resistance has become a major challenge in effective treatment. Owing to the versatile biological activity of the piperazine moiety, numerous antibacterial agents containing piperazine derivatives have been developed [51]. Preeti Chaudhary et al. [52] synthesized a series of substituted piperazine derivatives and evaluated their antimicrobial activity, where the synthesized compounds exhibited significant effectiveness against several bacterial strains. Similarly, K.S. Thriveni et al. [53] synthesized pyrimidine-incorporated piperazine compounds and investigated in vitro antibacterial activity against Gram-positive bacteria, including Staphylococcus aureus (NCIM2492) and Bacillus subtilis (NCIM2088), as well as Gram-negative bacteria such as Escherichia coli (NCIM2138) and Salmonella paratyphi-A (ATCC3220).

Piperazine derivatives exhibit broad pharmacological activities because of their flexible heterocyclic structure. Their anticancer properties are associated with mechanisms such as cell-cycle arrest, apoptosis induction, and inhibition of tumor-growth pathways, whereas their anti-inflammatory activity is mainly attributed to the suppression of cytokines, nitric oxide production, and inflammatory signaling mediators. These combined biological effects demonstrate the considerable therapeutic potential of piperazine-based compounds in pharmaceutical and medicinal chemistry.

4. Conclusions

This review summarizes recent advancements in nonlinear optical (NLO) single crystals, highlighting significant progress in crystal growth, structural characterization, and optical property analysis. Single-crystal X-ray diffraction (SCXRD) plays a key role in confirming the crystal structure, while UV–Visible–NIR spectroscopy provides insights into electronic transitions, chromophore behavior, and optical band-gap determination. These studies are essential for understanding the electronic structure and semiconducting nature of NLO materials.

Photoconductivity analysis further explains variations in electrical conductivity under light irradiation, which are governed by charge-carrier generation, recombination, and trapping mechanisms. In addition, laser damage threshold (LDT) studies indicate the suitability of crystals for high-power laser applications, optical coatings, and nonlinear optical devices. High LDT values suggest strong potential for operation in demanding environments such as laser fusion systems and industrial laser technologies.

The Z-scan technique confirms the presence of strong third-order nonlinear optical properties, including the nonlinear refractive index (n_2) and nonlinear absorption coefficient (β), demonstrating promising optical-limiting and all-optical switching behavior. The observed self-focusing effect and enhanced third-order nonlinear susceptibility (χ^3) further supports the applicability of these materials in high-intensity laser systems.

Overall, piperazine-based crystalline materials exhibit excellent structural stability and tunable optical properties, making them highly promising candidates for applications in nonlinear optics, photonics, and biomedicine, including drug delivery, biosensors, and tissue engineering. Future research should focus on optimizing crystal growth conditions, enhancing the NLO response, and investigating dopant effects to further improve their performance in advanced optical and photonic applications.

Acknowledgments

The authors would like to thank SAIF IIT-Madras for the single crystal X-ray diffraction analysis.

Funding Statement

One of the authors, Dr. Muthu Senthil Pandian, acknowledges the financial support from the Science and Engineering Research Board (SERB) (CRG/2022/002734) under the Core Research Grant (CRG). One of the author Dr. B. Sahaya Infant Lasalle, thanks SSN College of Engineering for providing Post Doctoral Fellow.

Data Availability Statements

The datasets generated and/or analyzed during the current study can be obtained from the corresponding author upon reasonable request.

Authors Contribution Statement

B. Sahaya Infant Lasalle: Conceptualization, Data curation, Writing – original draft.

M. Senthil Pandian: Project administration, Supervision, Validation.

P. Ramasamy: Validation

Conflicts of Interest

The authors submit the revised manuscript titled "A Comprehensive study on the Synthesis, Nonlinear Optical Properties, and Biological Applications of Substituted Piperazine Derivatives" for publication in your esteemed journal. The authors confirm that the manuscript is an original work, not under consideration by any other journal, and has not been previously published. The authors are fully familiar with the content of the manuscript and approve its submission. There are no conflicts of interest to disclose regarding this submission.

Data Availability

Data will be made available upon request.

References

[1] Rekha, P., Peramaiyan, G., NizamMohideen, M., Mohan Kumar, R., and Kanagadurai, R., 2015. Synthesis, growth, structural and optical studies of a novel organic Piperazine (bis) p-toluenesulfonate single crystal. *Spectrochimica Acta Part A: Molecular and Biomolecular Spectroscopy*, 139, pp.302–306.

[2] Perli, M., and Govindarajan, R., 2020. Piperazine derivatives: A review of biological activities. *World Journal of Pharmaceutical Research*, 9(14), pp.194-204.

[3] Sangeetha, G. P., Vijayaraghavan, G. V., and Priscilla, J., 2026. The effect of piperazine on hippuric acid single crystal growth and characterization for nonlinear optical applications. *Journal of Materials Science: Materials in Electronics*, 37(4), p.336.

[4] Klingshirn, C., 1990. Non-linear optical properties of semiconductors. *Semicond. Sci. Technol*, 5, p.457.

[5] Naseema, K., Shyma, M., Manjunatha, K. B., Muralidharan, A., Umesh, G., and Rao, V., 2011. χ(3) measurement and optical limiting studies of urea picrate. *Optics & Laser Technology*, 43, pp.1286–1291.

[6] Revathi Ambika, V., Jayalakshmi, D., Narendran, K., Athimoolam, S., Valan, M. F., Kamalarajan, P., and Irshad Ahamed, J., 2021. Growth, structural, spectral, optical and thermal studies of a novel third-order nonlinear optical single crystal: Piperazine-1,4-diium bis(2, 4-dichlorobenzoate). *Journal of Molecular Structure*, 1225, p.129292.

[7] Lasalle, B. S. I., Muthu, S. P., Anitha, K., and Ramasamy, P., 2023. Synthesis, crystal growth and characterization of piperazinium 5-nitrosalicylate (P5NS) single crystal for nonlinear optical (NLO) applications. *Journal of Molecular Structure*, 1286, p.135650.

[8] Lasalle, B. S. I., Pandian, M. S., Anitha, K., and Ramasamy, P., 2023. Growth of piperazinium bis(trifluoroacetate) (PTFA) single crystal for nonlinear optical (NLO) application. *J Mater Sci: Mater Electron*, 34, p.1527.

[9] Sahaya Infant Lasalle, B., Senthil Pandian, M., Anitha, K., and Ramasamy, P., 2023. Crystal growth and characterization of piperazinium mercuric chloride (PMC) single crystal for

nonlinear optical (NLO) application. *Inorganic Chemistry Communications*, 157, p.111397.

[10] Aswaniya, K., Raj, M. B. J., Gowri, S., and Vinitha, G., 2020. Growth, structural, hirshfeld surface analysis, DFT and Z-scan technique of hybrid single crystal of piperazinium perchlorate. *Journal of Molecular Structure*, 1218, p.128460.

[11] Pichan, K., Muthu, S. P., and Perumalsamy, R., 2017. Crystal growth and characterization of third order nonlinear optical piperazinium bis(4-hydroxybenzenesulphonate) (P4HBS) single crystal. *Journal of Crystal Growth*, 473, pp.39–54.

[12] Dhanalakshmi, B., Ponnusamy, S., Muthamizhchelvan, C., and Subhashini, V., 2015. Growth and characterization of Piperazinium adipate: A third order NLO single crystal. *Journal of Crystal Growth*, 426, pp.103–109.

[13] Subhashini, V., Ponnusamy, S., Muthamizhchelvan, C., and Dhanalakshmi, B., 2013. Growth and characterization of piperazinium 4-nitrophenolate monohydrate (PNP): A third order nonlinear optical material. *Optical Materials*, 35, pp.1327–1334.

[14] Subhashini, V., Ponnusamy, S., and Muthamizhchelvan, C., 2013. Synthesis, growth, spectral, thermal, mechanical and optical properties of piperazinium (meso)tartrate crystal: A third order nonlinear optical material. *Journal of Crystal Growth*, 363, pp.211–219.

[15] Rekha, P., Peramaiyan, G., NizamMohideen, M., Mohan Kumar, R., and Kanagadurai, R., 2015. Synthesis, growth, structural and optical studies of a novel organic Piperazine (bis) p-toluenesulfonate single crystal. *Spectrochimica Acta Part A: Molecular and Biomolecular Spectroscopy*, 139, pp.302–306.

[16] Lasalle, B. S. I., Kamalesh, T., Karuppasamy, P., Pandian, M. S., and Ramasamy, P., 2022. Investigation of growth, optical, thermal, mechanical, electrical, laser damage threshold properties of 1, 2, 3-Benzotriazolium Dihydrogen Phosphate (BTDHP) single crystal for nonlinear optical (NLO) applications. *J Mater Sci: Mater Electron*, 33, pp.24718–24733.

[17] Lasalle, B. S. I., Karuppasamy, P., Pandian, M. S., and Ramasamy, P., 2022. Investigation of structural, optical, and thermal properties of 2-amino-4,6-dimethylpyrimidine benzoic acid (2APB) single crystal for non-linear optical (NLO) applications. *J Mater Sci: Mater Electron*, 33, pp.17780–17792.

[18] Sahaya Infant Lasalle, B., Senthil Pandian, M., Anitha, K., and Ramasamy, P., 2023. Investigation of growth, optical, thermal, mechanical, electrical, laser damage threshold properties of 3-amino-1,2,4-triazolium benzoate (3ATB) single crystals for nonlinear optical applications. *J Mater Sci: Mater Electron*, 34, p.1714.

[19] Sahaya Infant Lasalle, B., Manikandan, A., Senthil Pandian, M., and Ramasamy, P., 2023. Theoretical and Experimental Investigation on 1,2,3-Benzotriazole 4-Hydroxybenzoic Acid (BTHBA) Single Crystals for Third-Order Nonlinear Optical (NLO) Applications. *Crystal Research and Technology*, 58, p.2200155.

[20] Arunpandian, R., Lasalle, B. S. I., Balagowtham, N., Krishnamachari, M., Pandian, M. S., Ramasamy, P., Mohanraj, K., Chiang, C.-H., and Yang, P.-Y., 2023. Computational and experimental investigation on piperazinediium bis (4-aminobenzoate) dihydrate single crystal for NLO applications. *Journal of Molecular Structure*, 1288, p.135811.

[21] Lasalle, B. S. I., Pandian, M. S., Anitha, K., and Ramasamy, P., 2023. Growth and characterization of organic NLO single crystal 1,2,3-Benzotriazole 4-chloro-2-Nitrobenzoic acid. *J Mater Sci: Mater Electron*, 34, p.1993.

[22] B., S. I. L., Muthu, S. P., K., P., G., B., and R., P., 2023. Synthesis, crystal growth and characterization of organic 1,2,4-triazole p-nitrophthalic acid (TPNP) single crystal for nonlinear optical (NLO) applications. *Inorganic Chemistry Communications*, 158, p.111549.

[23] Sahaya Infant Lasalle, B., Senthil Pandian, M., Karuppasamy, P., Sivasubramani, V., and Ramasamy, P., 2024. Comparative investigation on slow evaporation solution technique and Sankaranarayanan-Ramasamy (SR) method semi-organic Piperazinium Tetrachlorozincate Monohydrate (PTCZM) single crystal for optoelectronic applications. *J Mater Sci: Mater Electron*, 35, p.242.

[24] Sahaya Infant Lasalle, B., Senthil Pandian, M., Anitha, K., and Ramasamy, P., 2024. Single crystal growth of 1,2,3-Benzotriazole 3,5-dinitrobenzoic acid (BTNBA) by slow evaporation solution technique (SEST) for nonlinear optical (NLO) applications. *Inorganic Chemistry Communications*, 162, p.112190.

[25] Prasad, K. M., Srinivasan, P., Barik, S. K., Lasalle, B. S. I., Pandian, M., and Ramasamy, P., 2024. Studies on the synthesis, growth, and characterization of 2-cyanopyridinium salicylate single crystals for nonlinear optical applications. *Journal of Molecular Structure*, 1312, p.138468.

[26] Alexandar, A., Lasalle, B. S. I., Pandian, M. S., Girisun, T. C. S., and Vijayan, N., 2024. Growth and characterizations of anthracene single crystal for optical limiting and optoelectronics applications: a scintillation material. *J Mater Sci: Mater Electron*, 35, p.142.

[27] Alexandar, A., Lasalle, B. S. I., Pandian, M. S., Johnson, I., Rosario, S. R., Kavitha, G., and Girisun, T. C. S., 2024. Growth and optoelectronic characterizations of potassium hydrogen phthalate single crystals for two-photon absorption and optical limiting applications. *J Mater Sci: Mater Electron*, 35, p.1073.

[28] Karuppasamy, P., Kamalesh, T., Anitha, K., Abdul Kalam, S., Senthil Pandian, M., Ramasamy, P., Verma, S., and Venugopal Rao, S., 2018. Synthesis, crystal growth, structure and characterization of a novel third order nonlinear optical organic single crystal: 2-Amino 4,6-Dimethyl Pyrimidine 4-nitrophenol. *Optical Materials*, 84, pp.475–489.

[29] Lasalle, B. S. I., Pandian, M. S., Anitha, K., and Ramasamy, P., 2025. Development and characterization of a novel organic piperazinium-2-nitrobenzoate single crystal for optoelectronic applications. *Optical Materials*, p.117369.

[30] Lasalle, B. S. I., Muthu, S. P., Alexandar, A., Narmadha, S., Jeeva Govind, R., Kumar, M., and Chang, J.-H., 2025. Growth and functional characterization of piperazinium bis (sulfamate) single crystals for nonlinear optical and optoelectronic applications. *Solid State Communications*, p.116173.

[31] Turcicova, H., Novak, O., Muzik, J., Stepankova, D., Smrz, M., and Mocek, T., 2022. Laser induced damage threshold (LIDT) of β-barium borate (BBO) and cesium lithium borate (CLBO) – Overview. *Optics & Laser Technology*, 149, p.107876.

[32] Priscilla, J., Vijayaraghavan, G. V., and Lakshmipriya, M., 2024. Effect of laser irradiation on the growth of Adipic acid single crystal for NLO applications. *J Mater Sci: Mater Electron*, 35, p.1080.

[33] Sahaya Infant Lasalle, B., Muthu, S. P., Ghorui, C., Chaudhary, A. K., Karuppasamy, P., and Ramasamy, P., 2024. Growth and characterization of piperazinium bis(trifluoroacetate) (PTFA) single crystal for terahertz (THz) optoelectronic applications. *Optical Materials*, 148, p.114968.

[34] Hakkim, M. A. A., Paulraj, R., Bhatt, R., Soharab, M., Sidden, C., Bhaumik, I., and Perumalsamy, R., 2024. Directional growth of 2-ethylimidazolium d-tartrate crystal along (001) and investigation of optical properties for optical limiting applications. *Optical Materials*, 152, p.115421.

[35] Hakkim, A., Asikali, M., Paulraj, R., Sidden, C., and Perumalsamy, R., 2022. Study of the Crystalline perfection, homogeneity, chemical etching on the surface, and thirdorder nonlinear optical properties of (1 1 0) oriented hydroxyethylammonium D-tartrate monohydrate single crystal and hirshfeld surface analysis. *Cryst. Res. Technol*, 57, p.12.

[36] Sahaya Infant Lasalle, B., Senthil Pandian, M., Karuppasamy, P., and Ramasamy, P., 2024. Synthesis, crystal growth, structural, optical, and laser damage threshold characterizations on 2-amino-4,6-dimethyl-pyrimidinium hydrogen sulfate single crystal for nonlinear optical applications. *Materials Letters*, 356, p.135598.

[37] Ragu, R., Akilan, M., Angelena, J. P., Latha Mageshwari, P. S., and Das, S. J., 2019. Growth, optical, mechanical, thermo-physical, laser damage threshold (LDT) and Z-scan studies on dilithium succinate single crystal for optical limiting applications. *J Mater Sci: Mater Electron*, 30, pp.6287–6299.

[38] B., S. I. L., N., B., Muthu, S. P., P., K., and P., R., 2024. Experimental and theoretical investigation on the SR method grown semi-organic Piperazinium Tetrachlorozincate Monohydrate (PTZM) single crystal for optoelectronic applications. *Optik*, 309, p.171855.

[39] Shakir, M., Kushwaha, S. K., Maurya, K. K., Bhatt, R. C., Rashmi, Wahab, M. A., and Bhagavannarayana, G., 2010. Unidirectional growth of l-proline cadmium chloride monohydrate single crystal and its characterization for structural, vibrational, LDT, optical and dielectric properties. *Materials Chemistry and Physics*, 120, pp.566–570.

[40] John, N. L., Abraham, S., George, J., Karuppasamy, P., Senthilpandian, M., Ramasamy, P., and Vinitha, G., 2022. Synthesis, structure, NBO, Hirshfeld surface, NMR, HOMO-LUMO, UV, photoluminescence, z scan, vibrational and thermal analysis of piperazinedi-ium tetrakis (μ2-chloro)-diaqua-dichloro-di-cadmium single crystal. *Journal of Molecular Structure*, 1258, p.132685.

[41] Girase, P. S., Dhawan, S., Kumar, V., Shinde, S. R., Palkar, M. B., and Karpoormath, R., 2021. An appraisal of anti-mycobacterial activity with structure-activity relationship of piperazine and its analogues: A review. *European Journal of Medicinal Chemistry*, 210, p.112967.

[42] Sajadikhah, S. S., and Nassiri, M., 2021. Recent developments in the synthesis of piperazines (microreview). *Chem Heterocycl Comp*, 57, pp.905–907.

[43] Rasheed, A. M., Shetty, K. K., Roy, L. D., and Kumar, J., 2024. Novel Piperazine Derivatives as Potent Antihistamine, Anti-Inflammatory, and Anticancer Agents, their Synthesis and Characterization. *Anti-Cancer Agents in Medicinal Chemistry*, 24, pp.1063–1073.

[44] Khalili, F., Henni, A., and East, A. L. L., 2009. pKa Values of Some Piperazines at (298, 303, 313, and 323) K. *J. Chem. Eng. Data*, 54, pp.2914–2917.

[45] Lacivita, E., Leopoldo, M., Giorgio, P. D., Berardi, F., and Perrone, R., 2009. Determination of 1-aryl-4-propylpiperazine pKa values: The substituent on aryl modulates basicity. *Bioorganic & Medicinal Chemistry*, 17, pp.1339–1344.

[46] Bernstein, J., Davis, R. E., Shimoni, L., and Chang, N.-L., 1995. Patterns in Hydrogen Bonding: Functionality and Graph Set Analysis in Crystals. *Angewandte Chemie International Edition in English*, 34, pp.1555–1573.

[47] Goodman & Gilman's, 2004. The Pharmacological Basis of Therapeutics: Tenth Edition. *McGraw-Hill*.

[48] Ahmadi, A., Khalili, M., Hajikhani, R., Safari, N., and Nahri-Niknafs, B., 2012. Anti-inflammatory effects of two new methyl and morpholine derivatives of diphenhydramine on rats. *Med Chem Res*, 21, pp.3532–3540.

[49] Abu-Aisheh, M. N., Mustafa, M. S., El-Abadelah, M. M., Naffa, R. G., Ismail, S. I., Zihlif, M. A., Taha, M. O., and Mubarak, M. S., 2012. Synthesis and biological activity assays of some new N1-(flavon-7-yl)amidrazone derivatives and related congeners. *European Journal of Medicinal Chemistry*, 54, pp.65–74.

[50] Zhang, R.-H., Guo, H.-Y., Deng, H., Li, J., and Quan, Z.-S., 2021. Piperazine skeleton in the structural modification of natural products: a review. *Journal of Enzyme Inhibition and Medicinal Chemistry*, 36, pp.1165–1197.

[51] Shaquiquzzaman, M., Verma, G., Marella, A., Akhter, M., Akhtar, W., Khan, M. F., Tasneem, S., and Alam, M. M., 2015. Piperazine scaffold: A remarkable tool in generation of diverse pharmacological agents. *European Journal of Medicinal Chemistry*, 102, pp.487–529.

[52] Chaudhary, P., Kumar, R., Verma, A. K., Singh, D., Yadav, V., Chhillar, A. K., Sharma, G. L., and Chandra, R., 2006. Synthesis and antimicrobial activity of N-alkyl and N-aryl piperazine derivatives. *Bioorganic & Medicinal Chemistry*, 14, pp.1819–1826.

[53] Thriveni, K. S., Padmashali, B., Siddesh, M. B., and Sandeep, C., 2014. Synthesis of Pyrimidine Incorporated Piperazine Derivatives and their Antimicrobial Activity. *Indian J Pharm Sci*, 76, pp.332–338.